Single-Cell Characterization of ^{18}F-FLT Uptake with Radioluminescence Microscopy

Debanti Sengupta and Guillem Pratx

Department of Radiation Oncology, Stanford University School of Medicine, Palo Alto, California

The radiotracer 3′-deoxy-3′-^{18}F-fluorothymidine (^{18}F-FLT) is commonly used to measure cell proliferation in vivo. As a marker of cell proliferation, ^{18}F-FLT is expected to be differentially taken up by arrested and actively dividing cells, but PET measures only aggregate uptake by tumor cells and therefore the single-cell distribution of ^{18}F-FLT is unknown. We used a novel in vitro radioluminescence microscopy technique to measure the differential distribution of ^{18}F-FLT radiotracer with single-cell precision. **Methods:** Using radioluminescence microscopy, we imaged the absolute uptake of ^{18}F-FLT in live MDA-MB-231 cells grown under different serum conditions. We then compared ^{18}F-FLT uptake with a standard measure of cell proliferation, using fluorescence microscopy of 5-ethynyl-2′-deoxyuridine incorporation in fixed cells. **Results:** According to 5-ethynyl-2′-deoxyuridine staining, few cells (1%) actively cycled under serum deprivation whereas most of them (71%) did under 20% serum. The distribution of ^{18}F-FLT reflected this dynamic. At 0% serum, uptake of ^{18}F-FLT was heterogeneous but relatively low. At 20% serum, a subpopulation of ^{18}F-FLT–avid cells, representing 61% of the total population, emerged. Uptake of ^{18}F-FLT in this population was 5-fold higher than in the remainder of the cells. Such a dichotomous distribution is not typically observed with other radiotracers, such as ^{18}F-FDG. **Conclusion:** These results suggest that increased ^{18}F-FLT uptake by proliferating cells is due to a greater fraction of ^{18}F-FLT–avid cells rather than a change in ^{18}F-FLT uptake by individual cells. This finding is consistent with the fact that ^{18}F-FLT uptake is mediated by thymidine kinase 1 expression, which is higher in actively dividing cells. Overall, these findings suggest that, within the same patient, changes in ^{18}F-FLT uptake reflect changes in the number of actively dividing cells, provided other parameters remain the same.

Key Words: cancer proliferation; thymidine analogs; single cell radionuclide imaging

J Nucl Med 2016; 57:1136–1140
DOI: 10.2967/jnumed.115.167734

In this study, we investigated the cellular distribution of 3′-deoxy-3′-^{18}F-fluorothymidine (^{18}F-FLT) using radioluminescence microscopy, a novel radionuclide imaging method with single-cell resolution.

^{18}F-FLT is often used with PET to measure cancer proliferation in vivo, in a preclinical or clinical setting. However, the question of whether ^{18}F-FLT truly measures proliferation remains controversial. Although ^{18}F-FDG PET is extensively used for tumor mapping, PET studies with ^{18}F-FLT have been less reliable (*1–3*). Cellular proliferation is fundamentally driven by whether individual cells enter cell division or remain in an arrested state. Therefore, cellular proliferation is best estimated by measuring the fraction of cells that is actively advancing through the cell cycle. However, in vivo measurements using ^{18}F-FLT PET cannot provide this information because information about the state of an individual cell is lost to averaging during the measurement process. This effect may contribute to the difficulty in interpreting in vivo ^{18}F-FLT data.

Cell proliferation can be measured either by using labeled nucleoside analogs to find the rate of DNA replication or by probing cell-cycle–specific markers. Tritiated thymidine has long been used to measure incorporation of thymidine into DNA (*4*). In combination with microautoradiography, the method allows for the frequency of DNA-synthesizing cells to be determined in a semiquantitative fashion. However, microautoradiography of tritiated compounds is technically challenging because of the long half-life of ^{3}H and the preparation of autoradiographic emulsions.

A more commonly used method is the 5-bromo-2′-deoxyuridine assay, which can be incorporated into DNA during replication as a substitute for thymidine (*5*). More recently, 5-ethynyl-2′-deoxyuridine (EdU) has been used as a replacement for 5-bromo-2′-deoxyuridine because of a simplified detection system (*6*) and has become commercially available. However, these assays are typically terminal since the procedure calls for cell fixation. In addition, because 5-bromo-2′-deoxyuridine and EdU are mutagenic and cytotoxic, they cannot be used in humans (*7*). Thus, use of this probe is limited to terminal experiments, using relatively short exposures.

The S-phase fraction can also be measured using flow cytometry with DNA staining. Another popular approach is immunostaining using a marker of proliferation such as Ki-67, which is expressed only in actively cycling cells (*8–10*). More recently, Raman spectroscopy has also been used to measure cell proliferation in vitro (*11*).

^{18}F-FLT is the only available method to assess tumor proliferation noninvasively in humans, but its use has been hampered by its poor accuracy. ^{18}F-FLT uptake correlates with thymidine kinase 1 (TK1) activity (*12*), which is strongly dependent on the cell cycle (*13*). TK1 is most highly expressed during the S-phase of the cell cycle; thus, a proliferating tumor, with a higher frequency of cells in the S-phase, is expected to take up ^{18}F-FLT more avidly. Since ^{18}F-FLT is not incorporated into the DNA, ^{18}F-FLT can be used clinically without lasting toxicity. However, ^{18}F-FLT measurements have limited accuracy in vivo. For one, the competition between the thymidine salvage pathway (which ^{18}F-FLT measures) and de novo DNA synthesis (*14*) can complicate the analysis of ^{18}F-FLT PET scans. Further, tumors with high local thymidine

Received Oct. 6, 2015; revision accepted Mar. 11, 2016.
For correspondence or reprints contact: Guillem Pratx, Stanford University School of Medicine, 1050 Arastradero Rd., Palo Alto, CA 94304.
E-mail: pratx@stanford.edu
Published online Apr. 14, 2016.

concentrations are known to take up ^{18}F-FLT less avidly regardless of their proliferation status (*2*).

In this study, we used a single-cell imaging technique called radioluminescence microscopy to image the uptake of ^{18}F-FLT in a human breast-cancer cell line under different proliferation conditions. Radioluminescence microscopy can visualize the uptake of PET tracers in vitro, with single-cell resolution, in a multimodal microscopy environment that also includes fluorescence and bright-field imaging capabilities (*15,16*). Although the method has been applied to various radiotracers such as ^{18}F-9-[4-fluoro-3-(hydroxymethyl)butyl]guanine (*16*), ^{18}F-FDG (*15*), and radioimmunoconjugates, the uptake of ^{18}F-FLT has previously not been measured in single cells. With this study, we aimed to demonstrate that ^{18}F-FLT uptake is a specific marker of proliferation at the single-cell level. Given the cell-cycle–specific expression of TK1, we postulated that only a subpopulation of cells, which are actively replicating, will take up and retain ^{18}F-FLT. We also aimed to determine how these single-cell ^{18}F-FLT measurements compare with EdU incorporation measured by fluorescence microscopy. In this manner, we hoped to validate ^{18}F-FLT as a marker of proliferation from a single-cell perspective and determine how EdU imaging compares with clinically used ^{18}F-FLT. These data would both validate the use of ^{18}F-FLT as an in vitro imaging platform and provide a point of comparison between EdU measurements and clinically used ^{18}F-FLT.

MATERIALS AND METHODS

Radioluminescence Microscopy Setup

Radioluminescence imaging was performed using a bioluminescence microscope (LV200; Olympus) outfitted with a ×40/numerical aperture 1.3 oil objective (UPLFLN40XO; Olympus) and a deep-cooled electron-multiplying charge-coupled device (ImageEM C9100-14; Hamamatsu). All samples were imaged using 4 × 4 binning and an electron-multiplication gain of 1,200. Fluorescence imaging was performed on a DM6000B microscope (Leica) using a C11440 fluorescence camera (Hamamatsu) and a DFC450 bright-field camera (Leica), with ×20 magnification and an exposure time of 4 s.

Cell-Based Imaging Experiments

MDA-MB-231 human breast cancer cells were purchased from the American Type Culture Collection and cultured in DMEM (Gibco) medium supplemented with 10% fetal bovine serum. These cells were chosen for their high expression of TK1 and avid uptake of ^{18}F-FLT (*17*). Glass-bottom dishes were coated with fibronectin (10 μg/mL) for 1 h. The dish was then washed 3 times with phosphate-buffered saline, and 10^5 cells were seeded and left to adhere overnight. The next day, the medium was changed to the serum condition required, and the cells were grown for 48 h. Low-serum (0%) or high-serum (20%) conditions were established to respectively arrest or promote cell proliferation (*18,19*). Imaging was performed the following day. The 2 imaging protocols are summarized in Figure 1. For radioluminescence experiments, cells were incubated with ^{18}F-FLT (18 MBq/mL for 60 min) or ^{18}F-FDG (9 MBq/mL for 60 min after 30 min of glucose fasting). The cells were then washed 3 times with phosphate-buffered saline, and a 500-mm-thick scintillator (CdWO4, 2-face polished; MTI Corp.) was placed on top of the cells. For ^{18}F-FLT imaging of the cells, radioluminescence microscopy was used with a 15- to 20-min total exposure time, split into 12,000 frames (75–100 ms/frame). For efflux measurements, the same cells were imaged consecutively, with an hour between imaging. For ^{18}F-FDG imaging, the total exposure time was 50 min, split into 30,000 frames (100 ms/frame). For fluorescence experiments, an EdU imaging kit (C10337; Life Technologies) and corresponding protocol were used (20 mM EdU for 1 h at 37°C). Live–dead staining was performed using the EVOS FL cell imaging system and the ReadyProbes cell viability imaging kit (R37609; ThermoFisher).

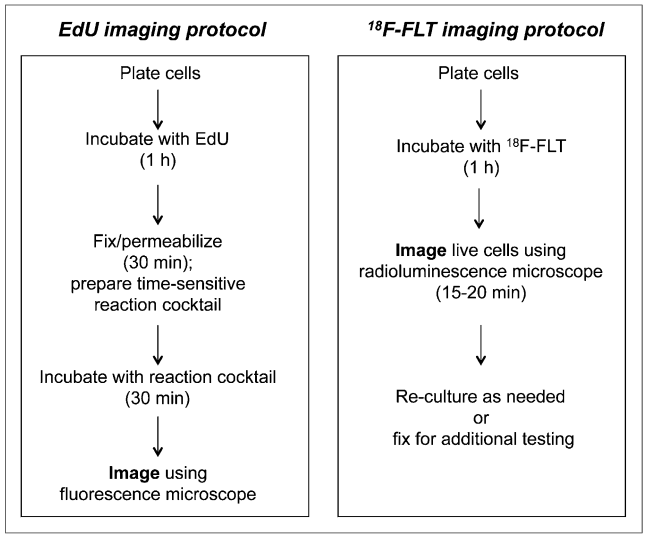

FIGURE 1. Comparison of steps to image cells with EdU or ^{18}F-FLT.

Image Analysis

Radioluminescence image reconstruction and analysis were performed using MATLAB (R2012b; The MathWorks). The raw camera frames were processed using our methodology called "optical reconstruction of the beta-ionization track," which is described in detail in a previous publication (*20*). Fluorescence micrographs were corrected for background effects by subtracting a dark image taken with a nonfluorescent sample and corrected for field flatness. Individual measurements of fluorescence or radioluminescence were obtained by manually placing circular regions of interest (diameter, 50 μm) on the bright-field micrograph, with similar regions of interest on the background as controls. Cell radiotracer uptake or fluorescent signal was defined as the total pixel intensity within the region of interest of the corrected images. Doublets or cell clusters were not quantified to avoid cross-talk between single cells. The number of molecules of ^{18}F-FLT was calculated using the number of observed decays per region of interest as previously detailed (*21*). For each image, a uniform background correction value was computed by placing regions of interest away from cells. For ^{18}F-FLT efflux measurements, the second set of measurements was decay-corrected using the decay time constant of ^{18}F. A gaussian mixture model was used to identify distinct clusters of cells with similar ^{18}F-FLT uptake from the radioluminescence images. Data fitting was performed in MATLAB using a maximum-likelihood expectation-maximization procedure.

RESULTS

In Figure 2, we compare radioluminescence-based ^{18}F-FLT imaging and fluorescence-based EdU imaging. Our first finding was that ^{18}F-FLT could be imaged in proliferating cells using radioluminescence microscopy, allowing us to produce high-quality images that demonstrate that the radiotracer is localized to individual cells. Furthermore, despite the limited spatial resolution of radioluminescence microscopy (typically 20–25 μm), the images suggested that ^{18}F-FLT was distributed throughout the cytoplasm,

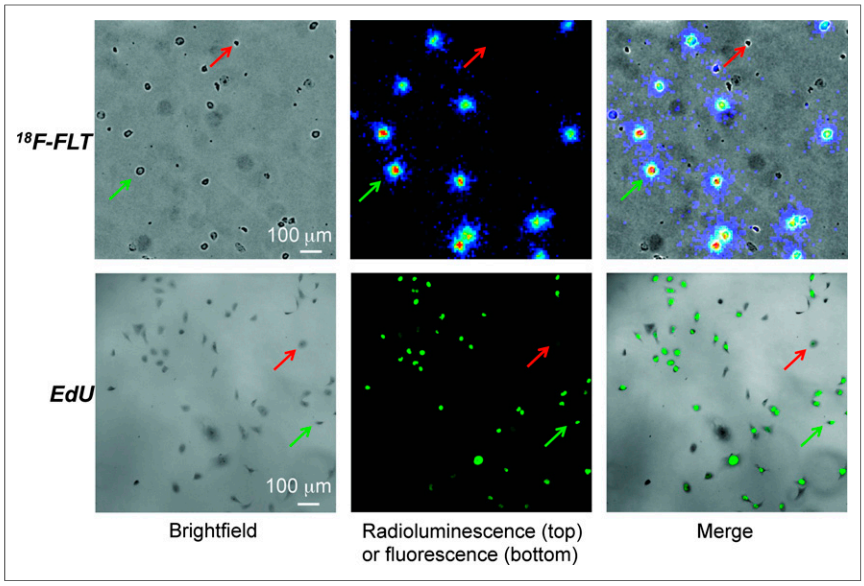

FIGURE 2. MDA-MB-231 cells imaged using ^{18}F-FLT and radioluminescence microscopy or EdU and fluorescence microscopy. Red and green arrows indicate cells with negative and positive signals, respectively.

as was expected since ^{18}F-FLT is not incorporated into the DNA. When a similar experiment was conducted using EdU, we observed that fluorescent microscopy could clearly identify individual cells that were in the S-phase of cell division. In contrast to ^{18}F-FLT, EdU was confined to the nucleus because the fixation and permeabilization steps of the staining protocol remove residual EdU from the cytoplasm. Fluorescence microscopy displayed higher image quality than radioluminescence microscopy, with notably better spatial resolution and lower noise.

We next attempted to determine whether radioluminescence imaging of ^{18}F-FLT uptake allows us to differentiate between cells that are proliferating rapidly and those that have undergone cell-cycle arrest. At the 0% serum condition, EdU staining was almost entirely negative, with fewer than 1% of cells stained; in contrast, at the 20% serum condition, 71% of cells produced a positive signal (Fig. 3). EdU imaging was thus able to effectively identify the subpopulation of cells that were in the S-phase of the cell cycle.

When ^{18}F-FLT uptake was quantified from radioluminescence images for arrested cells (0% serum), we observed a key difference between ^{18}F-FLT and EdU. Whereas EdU staining was almost entirely negative, uptake of ^{18}F-FLT was weak but above background for most of the arrested cells ($P < 0.001$; Fig. 3). The uptake of ^{18}F-FLT was heterogeneous in these cells, with a coefficient of variation of 77%. We separately verified that the starvation protocol did not result in significant cell death—93.6% ± 3.8% of cells cultured in 0% serum remained alive, as did 99.6% ± 0.1% of cells cultured in 20% serum.

For proliferating cells (20% serum), the frequency distribution of ^{18}F-FLT uptake in single cells appeared to be bimodal (Fig. 3). Using a gaussian mixture model, we automatically clustered the cells into 2 subpopulations based on their uptake of ^{18}F-FLT (Supplemental Fig. 1A; supplemental materials are available at http://jnm.snmjournals.org). We verified that the experimentally derived cumulative distribution function of ^{18}F-FLT uptake was well approximated by a 2-gaussian mixture model but not by a 1-gaussian function (Supplemental Fig. 1B).

The clustering of the gaussian mixture model yielded an equivalent threshold of 2,000 ^{18}F-FLT molecules per cell (≈0.2 Bq/cell). For the proliferating cells, the ^{18}F-FLT–high subpopulation displayed an average uptake of 5,300 molecules per cell, nearly 5-fold higher than the ^{18}F-FLT–low subpopulation (1,100 molecules per cell). The ^{18}F-FLT–low cell subpopulation was comparable in its uptake to the cells grown in 0% serum. Using the previously identified threshold, we observed that the number of ^{18}F-FLT–positive cells ranged from 8% under 0% serum conditions to 61% under 20% serum conditions.

Next, we compared the distribution of ^{18}F-FLT and ^{18}F-FDG uptake in the same cell line (Supplemental Fig. 2). The uptake by single cells was normalized by the mean uptake for an easier comparison. We found that although the uptake of ^{18}F-FDG followed a continuous distribution, with several cells concentrated around the mean, the ^{18}F-FLT data presented a distinctive bimodal distribution.

Finally, we evaluated efflux of ^{18}F-FLT from single proliferating cells (20% serum) over a 1-h period (Fig. 4). Regardless of actual ^{18}F-FLT uptake, we measured no significant efflux from the cells ($P > 0.6$). Consistent with previous measurements, we observed a cluster of cells with very low uptake and a second cluster representing 63% of the cells with higher uptake. This clustering was further verified using a gaussian mixture model to cluster the cells (data not shown).

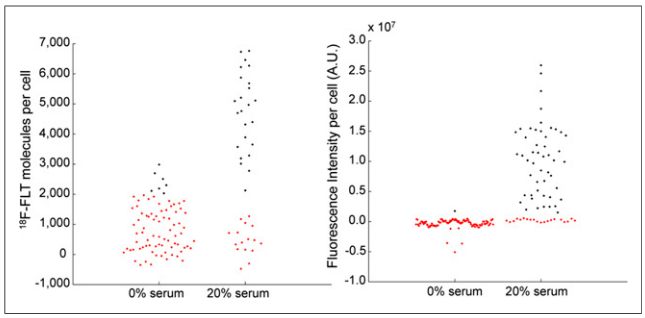

FIGURE 3. Quantification of individual cell signals from ^{18}F-FLT (left) and EdU (right). Each dot represents an individual cell. Red and black dots represent cells below and above signal threshold, respectively. A.U. = arbitrary units.

DISCUSSION

These results demonstrate that it is possible to image ^{18}F-FLT on a single-cell level and that ^{18}F-FLT is sensitive to the proliferation state of single cells. The side-by-side comparison with EdU demonstrated that the 2 probes measure similar proliferation processes in cells, since the frequency of positive cells was similar for ^{18}F-FLT and EdU. This single-cell side-by-side comparison of EdU and ^{18}F-FLT was valuable not just to validate the use of ^{18}F-FLT in a single-cell setting but also to create a point of comparison for EdU in conjunction with clinical uses of ^{18}F-FLT.

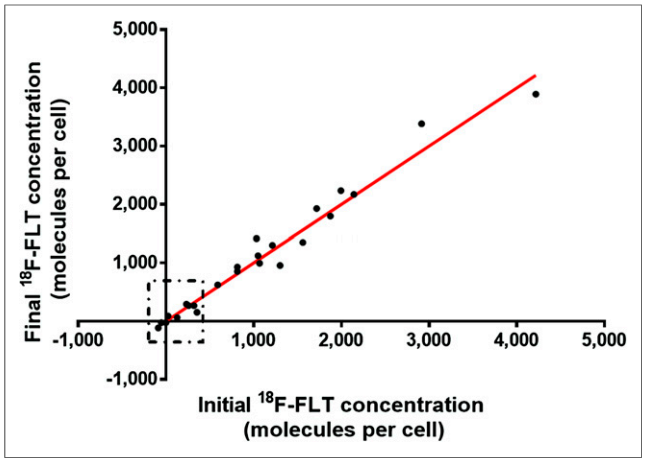

FIGURE 4. Single-cell ^{18}F-FLT uptake, measured shortly after removal of residual ^{18}F-FLT (*x*-axis) and 1 h later (*y*-axis). Each dot represents a single cell. Decay correction is applied. For reference, red line with slope of 1 is shown. Boxed region delineates ^{18}F-FLT–low subpopulation.

In any given cell population, only a certain number of cells will be dividing at any given time. Therefore, we expected only those cells to be taking up thymidine and thymidine analogs. We did observe this dichotomous distribution when studying ^{18}F-FLT uptake in proliferating cells (20% serum; Fig. 3). This phenomenon can be explained by the fact that TK1 expression is upregulated during the S-phase of the cell cycle and that therefore more ^{18}F-FLT is retained in cells that are actively dividing than in arrested cells. Such a dichotomous distribution is not typically observed with other tracers, such as ^{18}F-FDG.

The lack of detectable efflux from single cells over a 1-h period (Fig. 4) suggests that our single-cell assay measures only irreversibly trapped ^{18}F-FLT metabolites and, as a result, TK1 activity. Once taken up, ^{18}F-FLT is converted through TK1 and other downstream enzymes into ^{18}F-FLT-diphosphate and ^{18}F-FLT-triphosphate, both of which are resistant to degradation and efflux (*22*). Unbound ^{18}F-FLT likely flows out of the cell rapidly, before imaging starts, and therefore is not captured by this assay. Nucleoside transporters such as human equilibrative nucleoside transporters 1 and 2 or human concentrative nucleoside transporters 1 and 3 (*23*) may also modulate uptake of ^{18}F-FLT by increasing the intracellular availability of the probe, but it is unclear how significant this effect was in our experiment.

In vitro methods have previously been used to measure bulk ^{18}F-FLT uptake in cells and have demonstrated a good correlation of uptake with proliferation rate (*12*). In general, bulk measurements have important advantages. Because they can be done using millions of cells at a time, they generate lower technical noise than single-cell assays. They are also faster, have higher throughput, and are more standardized. However, single-cell measurements also confer some unique advantages. When the radiotracer uptake does not follow a single gaussian distribution, the average of all the cells, which is what is measured by a bulk assay, is not representative of the underlying characteristics of the population. This point is exemplified in our study of ^{18}F-FLT. Further, with single-cell measurements, there is no need for additional normalization to account for the concentration and viability of cells, as must be done in bulk sample measurements. Finally, single-cell measurements make it possible to measure radiotracer efflux for the exact same cell, over time, without requiring additional washing steps, which can cause significant cell loss.

It is important to note that TK1 levels will vary across cells in any given cell population, leading to heterogeneity in ^{18}F-FLT uptake. Overall, we find these intrapopulation variations to be smaller than the difference between arrested and proliferating cells. On average, ^{18}F-FLT uptake by proliferating cells is nearly 5-fold higher than that by arrested cells. Further, ^{18}F-FLT uptake in arrested cells does not significantly differ between the various serum conditions. Therefore, aggregate ^{18}F-FLT uptake, as measured on a PET scan, should be proportional to the frequency of actively cycling cells within the tumor. This, of course, is true only if all other parameters (e.g., per-cell TK1 expression and endogenous thymidine concentration) are the same.

We noticed above-background uptake even in serum-starved cells (Fig. 3), suggesting that TK1 has some basal level of activity even in noncycling cells (*12*). In contrast, EdU staining was virtually absent from arrested cells because cytoplasmic EdU is washed away during fixation and permeabilization and therefore only cells that incorporate EdU into their DNA display a positive signal, regardless of TK1 expression. This point is illustrated clearly in Figure 3, which shows that EdU uptake by arrested cells was densely clustered around 0 but that ^{18}F-FLT uptake was above background.

Another difference between EdU and ^{18}F-FLT is that the 2 nucleoside analogs are measured through very different physical processes. Because individual radionuclide decay can be detected with high sensitivity, EdU staining requires 20 mM EdU, which is approximately 7 orders of magnitude higher than the equivalent ^{18}F-FLT concentration needed for incubation (300 pM).

As previously mentioned, the EdU imaging protocol involves the intercalation of the EdU molecule into DNA and is therefore localized to the nucleus, whereas ^{18}F-FLT uptake simply measures the activity of TK1. Thus, the 2 assays are expected to produce related but different data. A key difference between the 2 methods is, of course, that the EdU protocol necessitates the fixation of cells before imaging whereas ^{18}F-FLT can image live cells directly, which allows time-course measurements (Fig. 4). On the other hand, the actual process of fluorescence image acquisition is significantly less time-intensive than radioluminescence image acquisition, which can take anywhere from 15 min to 1 h. Of course, the fluorescently labeled cells are also susceptible to photobleaching, and this can impact quantitation, but fixed cells can be mounted and saved for repeat analysis whereas cells incubated with ^{18}F-FLT must be imaged immediately. The 2 imaging modalities therefore offer specific advantages and disadvantages.

CONCLUSION

Our results show that increased uptake of ^{18}F-FLT by proliferating tumors is due to an increased fraction of ^{18}F-FLT–avid cells rather than a uniform change in ^{18}F-FLT uptake by individual cells. This finding is consistent with the fact that ^{18}F-FLT uptake is associated with TK1 expression, which is strong only in actively dividing cells. We have found similarities between data collected on a single-cell level using ^{18}F-FLT and EdU, and we have demonstrated that the distribution of ^{18}F-FLT is atypical and significantly different from other radiotracers, such as ^{18}F-FDG. Together, these results suggest that, within the same patient, changes in ^{18}F-FLT

uptake are reflective of changes in the number of actively dividing cells, provided that other parameters remain the same.

DISCLOSURE

The costs of publication of this article were defrayed in part by the payment of page charges. Therefore, and solely to indicate this fact, this article is hereby marked "advertisement" in accordance with 18 USC section 1734. The authors acknowledged funding from National Institutes of Health (NIH) grant R01CA186275 and support from the Stanford small-animal imaging facility and the Olympus Corporation for use of the LV200 microscope. No other potential conflict of interest relevant to this article was reported.

ACKNOWLEDGMENTS

We thank Prof. Frederick Chin and Dr. Zheng Miao from the Stanford radiochemistry facility, as well as Hongquan Li for assistance with image processing.

REFERENCES

1. Buck AK, Halter G, Schirrmeister H, et al. Imaging proliferation in lung tumors with PET: ^{18}F-FLT versus ^{18}F-FDG. *J Nucl Med.* 2003;44:1426–1431.
2. Zhang CC, Yan Z, Li W, et al. ^{18}F-FLT–PET imaging does not always "light up" proliferating tumor cells. *Clin Cancer Res.* 2012;18:1303–1312.
3. Troost EG, Vogel WV, Merkx MA, et al. ^{18}F-FLT PET does not discriminate between reactive and metastatic lymph nodes in primary head and neck cancer patients. *J Nucl Med.* 2007;48:726–735.
4. Sen-Oran E, Ozmen V, Bilir A, et al. Is the thymidine labeling index a good prognostic marker in breast cancer? *World J Surg Oncol.* 2007;5:93.
5. Thor AD, Liu S, Moore DH II, Edgerton SM. Comparison of mitotic index, in vitro bromodeoxyuridine labeling, and MIB-1 assays to quantitate proliferation in breast cancer. *J Clin Oncol.* 1999;17:470–477.
6. Salic A, Mitchison TJ. A chemical method for fast and sensitive detection of DNA synthesis in vivo. *Proc Natl Acad Sci USA.* 2008;105:2415–2420.
7. Diermeier-Daucher S, Clarke ST, Hill D, Vollmann-Zwerenz A, Bradford JA, Brockhoff G. Cell type specific applicability of 5-ethynyl-2′-deoxyuridine (EdU) for dynamic proliferation assessment in flow cytometry. *Cytometry A.* 2009;75:535–546.
8. Urruticoechea A, Smith IE, Dowsett M. Proliferation marker Ki-67 in early breast cancer. *J Clin Oncol.* 2005;23:7212–7220.
9. Keshgegian AA, Cnaan A. Proliferation markers in breast carcinoma: mitotic figure count, S-phase fraction, proliferating cell nuclear antigen, Ki-67 and MIB-1. *Am J Clin Pathol.* 1995;104:42–49.
10. Colozza M, Azambuja E, Cardoso F, Sotiriou C, Larsimont D, Piccart M. Proliferative markers as prognostic and predictive tools in early breast cancer: where are we now? *Ann Oncol.* 2005;16:1723–1739.
11. Wei L, Hu F, Shen Y, et al. Live-cell imaging of alkyne-tagged small biomolecules by stimulated Raman scattering. *Nat Methods.* 2014;11:410–412.
12. Rasey JS, Grierson JR, Wiens LW, Kolb PD, Schwartz JL. Validation of FLT uptake as a measure of thymidine kinase-1 activity in A549 carcinoma cells. *J Nucl Med.* 2002;43:1210–1217.
13. Munch-Petersen B, Cloos L, Jensen H, Tyrsted G. Human thymidine kinase 1. Regulation in normal and malignant cells. *Adv Enzyme Regul.* 1995;35:69–89.
14. Been LB, Suurmeijer AJ, Cobben DC, Jager PL, Hoekstra HJ, Elsinga PH. [^{18}F]FLT-PET in oncology: current status and opportunities. *Eur J Nucl Med Mol Imaging.* 2004;31:1659–1672.
15. Sengupta D, Miller S, Marton Z, Chin F, Nagarkar V, Pratx G. Bright Lu_2O_3:Eu thin-film scintillators for high-resolution radioluminescence microscopy. *Adv Healthc Mater.* 2015;4:2064–2070.
16. Pratx G, Chen K, Sun C, et al. Radioluminescence microscopy: measuring the heterogeneous uptake of radiotracers in single living cells. *PLoS One.* 2012;7:e46285.
17. Direcks WG, Berndsen S, Proost N, et al. [^{18}F]FDG and [^{18}F]FLT uptake in human breast cancer cells in relation to the effects of chemotherapy: an in vitro study. *Br J Cancer.* 2008;99:481–487.
18. Bell SP, Dutta A. DNA replication in eukaryotic cells. *Annu Rev Biochem.* 2002;71:333–374.
19. Jang B-C, Sanchez T, Schaefers H-J, et al. Serum withdrawal-induced post-transcriptional stabilization of cyclooxygenase-2 mRNA in MDA-MB-231 mammary carcinoma cells requires the activity of the p38 stress-activated protein kinase. *J Biol Chem.* 2000;275:39507–39515.
20. Pratx G, Chen K, Sun C, et al. High-resolution radioluminescence microscopy of ^{18}F-FDG uptake by reconstructing the β-ionization track. *J Nucl Med.* 2013;54:1841–1846.
21. Türkcan S, Nguyen J, Vilalta M, et al. Single-cell analysis of [^{18}F]fluorodeoxyglucose uptake by droplet radiofluidics. *Anal Chem.* 2015;87:6667–6673.
22. Grierson JR, Schwartz JL, Muzi M, Jordan R, Krohn KA. Metabolism of 3′-deoxy-3′-[F-18] fluorothymidine in proliferating A549 cells: validations for positron emission tomography. *Nucl Med Biol.* 2004;31:829–837.
23. Paproski RJ, Ng AM, Yao SY, Graham K, Young JD, Cass CE. The role of human nucleoside transporters in uptake of 3′-deoxy-3′-fluorothymidine. *Mol Pharmacol.* 2008;74:1372–1380.